Stationary light pulse in solids with long-lived spin coherence

Xiao-Jun Zhang,[1] Hai-Hua Wang,[1] Lei Wang,[1] Ren-Gang Wan,[1] Jun Kou,[1] Yun-Fei Fan,[1] Bing Zhang,[1,2] and Jin-Yue Gao[1,*]

[1]*College of Physics, Jilin University, Changchun 130023, People's Republic of China*

[2]*Mudanjiang Teachers' College, Mudanjiang 157012, People's Republic of China*

(Received 26 August 2010; published 7 June 2011)

We present a detailed analysis of stationary light pulses (SLP's) for the case of inhomogeneous broadening in both optical and spin transitions, which is normally found in solid materials with long-lived spin coherence. By solving the Langevin equations of motion for the density matrix elements under the integral over the entire range of the inhomogeneous broadenings, the necessary conditions for creating the SLP in a solid are obtained. Then the decay and diffusion processes that the SLP undergoes are analyzed. The characteristics of such processes are studied based on the analytic solution of the SLP with a slowly varying envelope. The dependence of SLP lifetime on inhomogeneous broadenings of spin and optical transitions, which can be regarded as the laser linewidth in the repump scheme, has been discussed.

DOI: 10.1103/PhysRevA.83.063804 PACS number(s): 42.50.Gy, 42.70.Qs, 42.50.Hz

I. INTRODUCTION

It is well known that if most atoms are on the lower level, a weak probe beam will be absorbed at its resonance frequency. However, by coupling an additional laser field; at the adjacent transition, the probe beam does not undergo an absorption process. This phenomenon has been referred to as electromagnetically induced transparency (EIT) [1]. The dispersion properties of the dressed samples are spatially homogeneously modified due to the external traveling-wave (TW) laser beam. Such schemes have led to many novel phenomena, such as adiabatic population and coherence transfer [2–4], resonant enhancement of optical nonlinearities [5–8], and the "storage of light," which means reversibly mapping the coherent excitation of the light into spin coherence [9–12]. Besides the traveling-wave coupled EIT (TW-EIT), the schemes with standing-wave driving EIT (SW-EIT) have also been widely studied [13–17]. Due to periodic modulation in space, such EIT samples can be exploited to manipulate the propagation of light, such as the realization of a tunable photonic bandgap [18–21] and the generation of a stationary light pulse (SLP) [22–25], which is actually a trapped light pulse with forward and backward components that can easily be stored and made to interchange. Owing to the important properties in nonlinear quantum optics, SLP's have been extensively studied. The SLP phenomenon has been demonstrated in both hot atomic gas [22] by Lukin *et al.* and cold ^{87}Rb atoms by Yu *et al.* [26].

Experiments on EIT in solids have been performed. With much higher laser intensities than those in a gaseous medium, transparency on the order of 100% can be achieved in rare-earth ion-doped crystals like Pr:YSO [27] and nitrogen-vacancy (N-V) centers in diamond [28–30]. A detailed theoretical analysis of EIT in solids was presented in Ref. [31]. Some interesting phenomena based on TW-EIT, such as all-optical routing [32,33], light storage [34–37], and enhanced four-wave mixing [38], just to mention a few, have also been demonstrated in solid materials. Motivated by practical considerations, we try to pursue the implementation of SLP's in solid materials, which have the obvious advantages, such as high density of atoms, compactness, convenience in preparation, the absence of atomic diffusion, and some disadvantages, such as broad optical lines and fast decoherence, which make it difficult for the realization of atomic interference. Although SLP's are very promising for the low-light-level nonlinear optics and the manipulation of photon states due to the increment of the interaction time between media and light, unfortunately, few investigations have been done on SLP's in solid materials.

The main aims of this paper are to clarify the following: (1) Is it possible to generate SLP's in inhomogeneously broadening solids with long-lived coherence, such as Pr:YSO, N-V centers in diamond, and some other rare-earth ion (Ce^{3+}, Eu^{2+}) doped crystals? (2) If it is possible, what are the characteristics of the decay dynamics for the SLP in these materials? In order to answer these questions, here we generalize the theory of SLP for the case of solids with long-lived coherence. The scheme of a four-level atomic system with a bichromatic SW coupling configuration is adopted in order to eliminate the counterpropagating Raman excitations which prohibit the formation of SLP's [26]. Section II lays the groundwork model for such a configuration as is needed to illustrate our general approach. It is then used in Sec. III to get the numerical results and analytic expressions of the SLP's in order to investigate SLP decay properties. In Sec. IV, we present our concluding remarks and a brief outlook.

II. THEORETICAL MODEL AND BASIC EQUATIONS

We consider an ensemble of double-Λ four-level atoms with two excited levels $|3\rangle$, $|4\rangle$ and two lower levels $|1\rangle$, $|2\rangle$. As shown in Fig. 1(a), the optical transitions with $|4\rangle - |2\rangle$ and $|3\rangle - |2\rangle$ are coupled by two lasers Ω_{c+} and Ω_{c-} with frequencies ν_{c+}, ν_{c-} and opposite wave vectors k_{c+}, k_{c-}. In the presence of a weak light pulse Ω_{p+} which has a frequency ν_{p+} at the resonance with $|1\rangle - |4\rangle$ transition and wave vector k_{p+} in the same direction of k_{c+}, a similar probe with wave vector k_{p-} determined by the phase-matching condition $k_{p-} = k_{p+} - k_{c+} + k_{c-}$ will be generated by four-wave mixing.

We define the Rabi frequencies for the coupling and probe fields as $\Omega_{c+(-)} = \mu_{42(32)}E_{c+(-)}/2\hbar$, $\Omega_{p+(-)} = \mu_{41(31)}E_{p+(-)}/2\hbar$, where $E_{c+(-)}$, $E_{p+(-)}$ are the amplitudes of the corresponding fields and μ_{ij} is the matrix element of the

*jygao@mail.jlu.edu.cn

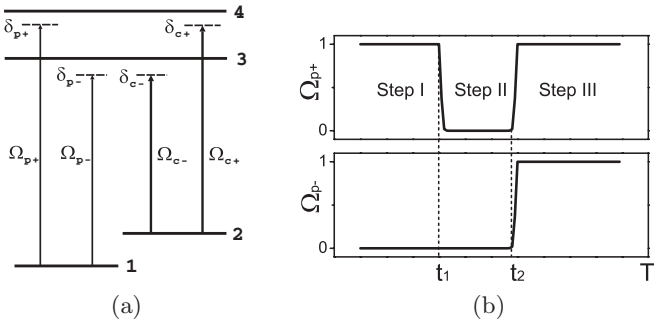

FIG. 1. (a) Energy-level schematic for the analysis. (b) Sequence of the coupling fields.

dipole moment between levels $|i\rangle$ and $|j\rangle$; it can be estimated as [31]

$$\mu_{ij}^2 = f\frac{e^2}{\hbar c}\frac{\hbar^2\lambda}{4\pi m_e}, \tag{1}$$

where f denotes the oscillator strength. As shown in Fig. 1(b), in the presence of Ω_{c+} in step I, the probe pulse Ω_{p+} moves slowly in the sample. In the following step, Ω_{c+} is adiabatically switched off, and the probe field Ω_{p+} (or parts of it) is stored in the sample as the spin coherence. At the beginning of step III, both coupling fields Ω_{c+} and Ω_{c-} are switched on, and the spin coherence is converted into Ω_{p+} and Ω_{p-}, which are the two components of the SLP. If the condition $\Omega_{p+} = \Omega_{p-}$ is satisfied, which means that the probability of the photons traveling forward equals that of traveling backward, the SLP is created.

In the usual electric-dipole and rotating-wave approximations, the dynamics of atomic population and coherence for the system is governed by a set of Langevin equations for the density elements given by Eqs. (2)–(10), where Γ_{ij} and γ_{ij} denote the population decay rate and the coherence decay rate, respectively:

$$\partial_t\rho_{11} = \Gamma_{31}\rho_{33} + \Gamma_{41}\rho_{44} + \Gamma_{21}\rho_{22} + ie^{-ikz}(\rho_{41}\Omega_{p+}^* - \rho_{13}\Omega_{p-}) - ie^{ikz}(\rho_{14}\Omega_{p+} + \rho_{31}\Omega_{p-}^*), \tag{2}$$

$$\partial_t\rho_{22} = \Gamma_{32}\rho_{33} + \Gamma_{42}\rho_{44} - \Gamma_{21}\rho_{22} + ie^{-ikz}(\rho_{42}\Omega_{c+}^* - \rho_{24}\Omega_{c+}) + ie^{ikz}(\rho_{32}\Omega_{c-}^* - \rho_{23}\Omega_{c-}), \tag{3}$$

$$\partial_t\rho_{33} = \Gamma_{43}\rho_{44} - \Gamma_{31}\rho_{33} - \Gamma_{32}\rho_{33} + ie^{-ikz}(\rho_{13}\Omega_{p-} + \rho_{23}\Omega_{c-}) - ie^{ikz}(\rho_{32}\Omega_{c-}^* - \rho_{31}\Omega_{p-}^*), \tag{4}$$

$$\partial_t\rho_{41} = (-\gamma_{41} + i\delta_{p+})\rho_{41} - ie^{-ikz}\Omega_{p-}\rho_{43} + ie^{ikz}[\Omega_{c+}\rho_{21} + \Omega_{p+}(\rho_{11} - \rho_{44})], \tag{5}$$

$$\partial_t\rho_{31} = (-\gamma_{31} + i\delta_{p-})\rho_{31} + ie^{-ikz}(\Omega_{c-}\rho_{21} - \Omega_{p-}\rho_{33} + \Omega_{p-}\rho_{11}) - ie^{ikz}\Omega_{p+}\rho_{34}, \tag{6}$$

$$\partial\rho_{42} = (-\gamma_{42} + i\delta_{c+})\rho_{42} - ie^{-ikz}\Omega_{c-}\rho_{43} + ie^{ikz}[\Omega_{p+}\rho_{12} + \Omega_{c+}(\rho_{22} - \rho_{44})], \tag{7}$$

$$\partial_t\rho_{32} = (-\gamma_{32} + i\delta_{c-})\rho_{32} + ie^{-ikz}(\Omega_{p-}\rho_{12} + \Omega_{c-}\rho_{22} - \Omega_{c-}\rho_{33}) - ie^{ikz}\Omega_{c+}\rho_{34}, \tag{8}$$

$$\partial_t\rho_{21} = [-\gamma_{21} + i\delta]\rho_{21} + e^{-ikz}(-\Omega_{p-}\rho_{23} + \Omega_{c+}^*\rho_{41}) - e^{ikz}(\Omega_{p+}\rho_{24} - \Omega_{c-}^*\rho_{31}), \tag{9}$$

$$\partial_t\rho_{43} = [-\gamma_{43} + i(\delta_{p+} - \delta_{p-})]\rho_{43} + e^{ikz}(\Omega_{p+}\rho_{13} + \Omega_{c+}\rho_{23} - \Omega_{p-}^*\rho_{41} - \Omega_{c-}^*\rho_{42}). \tag{10}$$

The detunings of the coupling fields $\delta_{c+(-)}$ are given by $\delta_{c+(-)} = \omega_{42(32)} - \nu_{c+(-)}$, and the detunings of the probe fields are $\delta_{p+(-)} = \omega_{41(31)} - \nu_{p+(-)}$. The parameter δ is $\delta_{p+} - \delta_{c+}$, which also equals $\delta_{p-} - \delta_{c-}$ based on the phase-matching condition mentioned previously. In the present analysis, the following assumptions are made to simplify our calculations: (i) $\Gamma_{41} = \Gamma_{42} = \Gamma_{31} = \Gamma_{32} = \Gamma$, $\gamma_{41} = \gamma_{42} = \gamma_{31} = \gamma_{32} = \gamma$, $\gamma_{43} = \gamma_{21} = \gamma_0$. (ii) The intensities of the coupling fields are much larger than those of the probe fields, so nearly all the ions interacting with the fields are on the ground level $|1\rangle$ ($\rho_{11} = 1$, $\rho_{22} = \rho_{33} = \rho_{44} = 0$). Associated with this assumption, the coherences between the transitions of $|4\rangle - |3\rangle$, $|4\rangle - |2\rangle$, and $|3\rangle - |2\rangle$ are neglectable. Under the above assumptions, we redefine the reset off-diagonal density elements as $\rho_{41} = \sigma_{41}e^{ikz}$, $\rho_{31} = \sigma_{31}e^{ikz}$, $\rho_{21} = \sigma_{21}e^{-2ikz}$, $\sigma_{ij} = \sigma_{ji}^*$. Then, the density equations become

$$\partial_t\sigma_{41} = -\sigma_{41}\tilde{\gamma}_{41} + i\Omega_{p+} + i\sigma_{21}\Omega_{c+}, \tag{11}$$

$$\partial_t\sigma_{31} = -\sigma_{31}\tilde{\gamma}_{31} + i\Omega_{p-} + i\sigma_{21}\Omega_{c-}, \tag{12}$$

$$\partial_t\sigma_{21} = -\sigma_{21}\tilde{\gamma}_{21} + i\sigma_{41}\Omega_{c+}^* + i\sigma_{31}\Omega_{c-}^*, \tag{13}$$

where $\tilde{\gamma}_{41} = \gamma - i\delta_{p+}$, $\tilde{\gamma}_{31} = \gamma - i\delta_{p-}$, $\tilde{\gamma}_{21} = \gamma_0 - i\delta$. In the following discussion, we focus on step III shown in Fig. 1(b) and assume that $\Omega_{c+} = \Omega_{c-} = \Omega_c$. As we know that the decoherence rate γ^{-1} is faster than the temporal changes of fields $\partial/\partial t$ [9], we can neglect $\partial_t\sigma_{31}$ and $\partial_t\sigma_{41}$ to get the zeroth solutions of σ_{31} and σ_{41}, which are

$$\sigma_{41}^{(0)} = i[\Omega_{p+}(z,t) + \Omega_c(z,t)\sigma_{21}]/\tilde{\gamma}_{41}, \tag{14}$$

$$\sigma_{31}^{(0)} = i[\Omega_{p-}(z,t) + \Omega_c(z,t)\sigma_{21}]/\tilde{\gamma}_{31}. \tag{15}$$

By substituting Eqs. (14) and (15) into Eq. (13), the equation of motion for the coherence σ_{21} and its zeroth-order solution can be written as

$$\frac{\partial\sigma_{21}}{\partial t} = -\frac{\Omega_+^2(z,t)}{\tilde{\gamma}_{41}} - \frac{\Omega_-^2(z,t)}{\tilde{\gamma}_{31}} \times \left[-\tilde{\gamma}_0 - \frac{\Omega_c^2(z,t)}{\tilde{\gamma}_{41}} - \frac{\Omega_c^2(z,t)}{\tilde{\gamma}_{31}}\right]\sigma_{21}, \tag{16}$$

$$\sigma_{21}^{(0)} = \frac{-\tilde{\gamma}_{31}\Omega_+^2(z,t) - \tilde{\gamma}_{41}\Omega_-^2(z,t)}{4\tilde{\gamma}_{21}\tilde{\gamma}_{31}\tilde{\gamma}_{41} + (\tilde{\gamma}_{31} + \tilde{\gamma}_{41})\Omega_c^2(z,t)}, \tag{17}$$

where $\Omega_+^2 = \Omega_{p+}\Omega_{c+}$, $\Omega_-^2 = \Omega_{p-}\Omega_{c-}$. The zeroth-order solutions are based on the approximation that the probe pulses have a very large length as compared with the length of the sample; therefore it can be regarded as a plane wave when it is

traveling through the medium. In order to describe the group velocities of the probe fields we need the first-order solution of σ_{21}. By inserting Eq. (17) into the time-derivative part of Eq. (16), we obtain

$$\sigma_{21} = \left[\frac{\partial\sigma_{21}^{(0)}}{\partial t} + \frac{\Omega_+^2(z,t)}{\tilde{\gamma}_{41}} + \frac{\Omega_-^2(z,t)}{\tilde{\gamma}_{31}}\right] \Big/ \times \left[-\tilde{\gamma}_0 - \frac{\Omega_c^2(z,t)}{\tilde{\gamma}_{41}} - \frac{\Omega_c^2(z,t)}{\tilde{\gamma}_{31}}\right]. \quad (18)$$

By substituting Eq. (18) into Eqs. (14) and (15), we find the expressions for the first-order solution of σ_{41} and σ_{31} given by

$$\sigma_{41} = \alpha_{1,3}\,\Omega_{p+}(z,t) + \alpha_2\,\Omega_{p-}(z,t) + \alpha_{3,3}\,\partial_t\Omega_{p+}(z,t) + \alpha_4\,\partial_t\Omega_{p-}(z,t), \quad (19)$$

$$\sigma_{31} = \alpha_2\,\Omega_{p+}(z,t) + \alpha_{1,4}\,\Omega_{p-}(z,t) + \alpha_4\,\partial_t\Omega_{p+}(z,t) + \alpha_{3,4}\,\partial_t\Omega_{p-}(z,t), \quad (20)$$

where

$$\alpha_{1,j} = -iA^{-3}B\tilde{\gamma}_{j1}^2\Omega_c(z,t)\,\partial_t\Omega_c(z,t) + iA^{-1}\left[\tilde{\gamma}_{21}\tilde{\gamma}_{j1} + \Omega_c^2(z,t)\right], \quad (21)$$

$$\alpha_2 = -iA^{-3}B\tilde{\gamma}_{31}\tilde{\gamma}_{41}\Omega_c(z,t)\,\partial_t\Omega_c(z,t) - iA^{-1}\Omega_c^2(z,t), \quad (22)$$

$$\alpha_{3,j} = iA^{-2}\tilde{\gamma}_{j1}^2\Omega_c^2(z,t), \quad (23)$$

$$\alpha_4 = iA^{-2}\tilde{\gamma}_{31}\tilde{\gamma}_{41}\Omega_c^2(z,t). \quad (24)$$

Here we have introduced two complex parameters, $A = \tilde{\gamma}_{21}\tilde{\gamma}_{31}\tilde{\gamma}_{41} + (\tilde{\gamma}_{31} + \tilde{\gamma}_{41})\,\Omega_c^2$ and $B = -\tilde{\gamma}_{21}\tilde{\gamma}_{31}\tilde{\gamma}_{41} + (\tilde{\gamma}_{31} + \tilde{\gamma}_{41})\,\Omega_c^2$, to simplify the above expressions. It is helpful to make some remarks on the properties of Eqs. (19) and (20), which describe the atomic polarizations of a group of ions defined by the detunings $\{\delta_{p+},\delta_{p-},\delta\}$ in the total frequency distributions of the solid materials. In the limit situation when the coupling fields Ω_{c+} and Ω_{c-} are simultaneously switching on at the very beginning of step III shown in Fig. 1(b), the components of the SLP are retrieved by the coupling fields. Such a process is directly related to the first term on the right-hand sides of Eqs. (21) and (22), which are proportional to $\partial_t\Omega_c$. In order to establish the stationary light pulse, those two terms must be equal, which leads to the first condition to generate the SLP:

$$\delta_{p+} = \delta_{p-}. \quad (25)$$

Considering the phase-matched condition, the condition can be regarded as the same condition as $\delta_{c+} = \delta_{c-}$, which implies that the two coupling fields drive the corresponding transitions with the same detunings and, as we assumed before, the same Rabi frequencies. It is natural that such conditions come up according to the pulse-matching phenomenon in EIT [39], and it is important for the following calculations.

In a solid system, both optical and spin transitions are inhomogeneously broadened due to the inhomogeneity of the crystalline field. The broadenings of the optical transitions $|4\rangle - |1\rangle$, $|3\rangle - |1\rangle$ and the spin transition $|2\rangle - |1\rangle$ are shown in Fig. 2(a). We assume that all the lasers are resonant with the line centers of the corresponding transitions. The energy levels for an ion we choose arbitrarily are denoted by solid horizontal lines in Fig. 2(a), and the relation between the laser and this chosen ion is just like what is shown in Fig. 1(a).

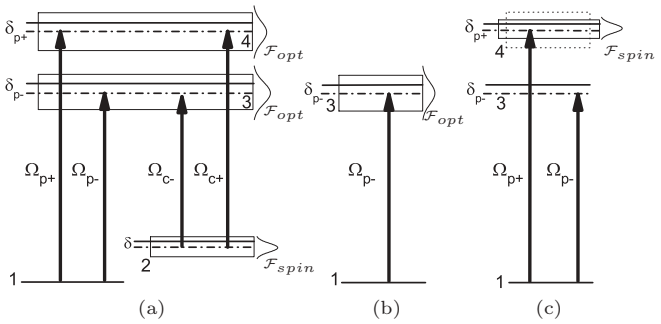

FIG. 2. Schematic level diagram of a four-level system with optical and spin inhomogeneous broadenings. (a) The rectangles denote the inhomogeneous broadenings for the transitions from the corresponding level to the level $|1\rangle$. The dash-dotted lines denote the broadening line centers, and the solid lines denote energy levels of an arbitrary ion we choose. We assume that all the lasers are assumed to be resonant with the line centers of the corresponding transitions. (b) The inhomogeneous broadening of the transition $|3\rangle - |1\rangle$. We treat it as the optical broadening. (c) The inhomogeneous broadening of the transition $|4\rangle - |1\rangle$. After the broadening of $|3\rangle - |1\rangle$ have been taken into account, as shown in (b), the broadening of $|4\rangle - |1\rangle$ is no longer considered as optical broadening but the spin broadening. For the ions with the same energy level $|3\rangle$ (no rectangle for $|3\rangle$), the frequency distribution is determined by the broadening of $|4\rangle - |3\rangle$ (solid rectangle). Such a model is based on the assumption that the spin broadening is always much smaller than the optical broadening. The dotted rectangle denotes the optical broadening of $|4\rangle - |1\rangle$ if all the ions are under consideration.

In order to describe the changes which are induced by such broadenings, we have to average σ_{41} and σ_{31} over the frequency distributions independently to get the total atomic polarizations:

$$\Sigma_{41(31)} = \iiint \mathcal{F}(\delta,\delta_{p+},\delta_{p-})\sigma_{41(31)}(\delta,\delta_{p+},\delta_{p-})\,d\delta\,d\delta_{p+}\,d\delta_{p-}. \quad (26)$$

The frequency distribution can be written as

$$\mathcal{F}(\delta,\delta_{p+},\delta_{p-}) = \mathcal{F}_{\rm spin}(\delta)\mathcal{F}_{\rm opt}(\delta_{p-})\mathcal{F}_{\rm spin}(\delta_{p+}), \quad (27)$$

where the spin (optical) frequency distribution function is denoted by $\mathcal{F}_{\rm spin}$ ($\mathcal{F}_{\rm opt}$).

The inhomogeneous broadening of transition $|2\rangle - |1\rangle$, namely, the spin broadening, is denoted by $\mathcal{F}_{\rm spin}(\delta)$. For the solid materials with long-lived spin coherence, the width of the spin broadening is relatively small, usually several kilohertz. The function $\mathcal{F}_{\rm opt}(\delta_{p-})$ corresponds to the broadening of the transition $|3\rangle - |1\rangle$ which is treated as the optical broadening as shown in Fig. 2(b). The optical broadening width is quite large for the relevant materials (2 GHz for Pr:YSO, 375 GHz for N-V centers in diamond); however, as reported in Ref. [27], not all of the ions in the solid can interact with the laser fields, but only a small fraction of them. This is due to the fact that a repump field is used to prepare the system, so the optical broadening

is very small, and mainly contributed by the laser linewidth (usually 1 MHz). The broadening of the transition $|4\rangle - |1\rangle$ is considered a spin broadening and denoted by $\mathcal{F}_{\rm spin}(\delta_{p+})$ in Eq. (27). The physical reason for such treatment as shown in Fig. 2(c) is that for the ions which have the same value of δ_{p-} (in another words, the same energy level of $|3\rangle$), the level $|4\rangle$ of those ions are distributed over a small range because of the inhomogeneous broadening of the transition $|4\rangle - |3\rangle$, which could be regarded as the same as that of the spin transition $|2\rangle - |1\rangle$. So, after we treat the broadening of $|3\rangle - |1\rangle$ as the optical broadening, the broadening of $|4\rangle - |1\rangle$ should be taken as the small spin broadening. This also means that for the ions with the same detuning δ_{p-}, the detuning δ_{p+} varies over a small range instead of being equal to δ_{p-}, so condition (25) cannot be satisfied. However, if the broadening of the spin transition is much smaller than the laser linewidth of the coupling fields, e.g., in Pr:YSO, the spin transition broadening is about 30 kHz, and the linewidth of the coupling field is normally 1 MHz. Condition (25) can be satisfied roughly. Therefore, we can disregard $|3\rangle - |4\rangle$ broadening by setting $\mathcal{F}_{\rm opt}(\delta_{p+}) = 1$, which means that ω_{43} is of the same value for all the ions, and the transition frequency of $|4\rangle - |1\rangle$ is fully determined by the transition frequency of $|3\rangle - |1\rangle$. But the inhomogeneous broadening of $|1\rangle - |2\rangle$ is still taken into account, because most ions are on these levels.

We adopt the Lorentzian function

$$\mathcal{F}_{\rm spin(opt)}(x) = \frac{w_{\rm spin(opt)}}{\pi\left(w^2_{\rm spin(opt)} + x^2\right)} \tag{28}$$

to model the inhomogeneous broadenings. Where the parameter $w_{\rm spin(opt)}$ is the width of the inhomogeneously broadening for the spin (optical) transition. Using the theorem of residues, the results of Eq. (26) can be obtained easily:

$$\begin{aligned}\Sigma_{41} = {} & \beta_1\,\Omega_{p+}(z,t) + \beta_2\,\Omega_{p-}(z,t) \\ & + \beta_3\,\partial_t\Omega_{p+}(z,t) + \beta_4\,\partial_t\Omega_{p-}(z,t),\end{aligned} \tag{29}$$

$$\begin{aligned}\Sigma_{31} = {} & \beta_2\,\Omega_{p+}(z,t) + \beta_1\,\Omega_{p-}(z,t) \\ & + \beta_4\,\partial_t\Omega_{p+}(z,t) + \beta_3\,\partial_t\Omega_{p-}(z,t),\end{aligned} \tag{30}$$

where[1]

$$\begin{aligned}\beta_1 = {} & -i\left[2\Omega_c^2(z,t) - G_{\rm opt}G_{\rm spin}\right] \\ & \times P^{-3}\Omega_c(z,t)\partial_t\Omega_c(z,t) + iG^{-1}_{\rm opt},\end{aligned} \tag{31}$$

$$\begin{aligned}\beta_2 = {} & -i\left[2\Omega_c^2(z,t) - G_{\rm spin}G_{\rm opt}\right] \\ & \times P^{-3}\Omega_c(z,t)\partial_t\Omega_c(z,t),\end{aligned} \tag{32}$$

$$\beta_3 = iP^{-2}\Omega_c^2(z,t), \tag{33}$$

$$\beta_4 = iP^{-2}\Omega_c^2(z,t). \tag{34}$$

The parameters $G_{\rm spin} = w_{\rm spin} + \gamma_0$, $G_{\rm opt} = w_{\rm opt} + \gamma$ can be regarded as the total decoherence rates of the spin and optical transitions, respectively. Because we choose the Lorentzian function to model the inhomogeneous broadening line shape, the total decoherence rates appear simply as the summation of the inhomogeneous broadening widths and the decoherence rate of the corresponding transitions. On the other hand, the Gaussian function which is indeed more accurate for the inhomogeneous broadening line shape will lead to much more complex results and a less clear physical picture on the effect of the broadenings. The parameter $P = G_{\rm spin}G_{\rm opt} + 2\Omega_c^2(z,t)$ is just used to simplify the above expressions.

After the inhomogeneous broadenings have been taken into account, the wave equations which describe the motion of two probe pulses can be used to analyze the system,

$$\frac{\partial\Omega_{p+}}{c\,\partial t} + \frac{\partial\Omega_{p+}}{\partial z} = ig\Sigma_{41}, \tag{35}$$

$$\frac{\partial\Omega_{p-}}{c\,\partial t} - \frac{\partial\Omega_{p-}}{\partial z} = ig\Sigma_{31}. \tag{36}$$

Here $g = 4\pi\nu N_{\rm eff}\,\mu^2/(\hbar\,c)$, ν is the transition frequency, μ is the dipole moment, and $N_{\rm eff}$ is the effective density of atoms depending on the laser linewidth $\Delta_{\rm jit}$. If the density of the atoms is N, the effective density should be $N_{\rm eff} = N\Delta_{\rm jit}/w_{\rm opt}$ [31]. This is because of the use of an optical repump scheme, as was done in Ref. [27].

Equations (29)–(36) are our main results, and could be applied in a rather general fashion when the SLP in the four-level inhomogeneously broadened system is to be investigated. It is worth mentioning that the four parameters (β_1, β_2, β_3, β_4) can describe the main properties of the system. First, β_1 and β_2 are responsible for the retrieval process at the beginning of step III shown in Fig. 1(b). After inserting Eqs. (31) and (32) into Eqs. (35) and (36), it is clear that the condition

$$\Omega_c \gg \sqrt{\frac{G_{\rm opt}G_{\rm spin}}{2}} \tag{37}$$

must be satisfied in order to convert the coherence back into photonic excitation. Note that this condition is quite similar to the EIT condition for the samples without any broadenings.

The parameters β_3 and β_4 which stand for the coefficients of $\partial_t\Omega_{p+}$ and $\partial_t\Omega_{p-}$ are of the same value; such a property directly results from the assumption $\gamma_{31} = \gamma_{41}$ and $\delta_{p+} = \delta_{p-}$ and is quite important for pulse matching of the SLP's components. Apparently, if there is a tendency that the two components are deviating from each other ($\partial_t\Omega_{p+} \neq \partial_t\Omega_{p-}$), it will be averaged by the polarizations so that the SLP can survive in the sample.

Then, as the answer to the first question we raised in Sec. I, we come to the following conclusion: It is possible to generate the SLP in solid materials as long as (i) the decoherence rates of the optical transitions are of the same magnitude, (ii) the broadening width of the spin transition is small enough that the condition of $\delta_{p+} = \delta_{p-}$ can be satisfied approximately, and (iii) the coupling fields are strong enough to satisfy condition (37).

Based on the above conclusions, we believe that the suitable solid materials are Pr^{3+}:Y_2SiO_5, N-V centers in diamond, and Eu^{2+}-doped crystals like Eu^{2+}:CaF_2, Eu^{2+}:SrF_2. On the other hand, Ce^{3+}-doped crystals (Ce^{3+}:YAG, Ce^{3+}:$LuPO_4$,

[1]Here the expressions of β_1 and β_2 have already been simplified. The neglected term is $-i(PG_{\rm opt})^{-1}\,\Omega_c^2(z,t)$, whose absolute value is much smaller than that of $iG_{\rm opt}$ on the basis of $G_{\rm spin} \ll G_{\rm opt}$.

TABLE I. The experimental parameters of Pr:YSO. λ is the wavelength of the laser field. The wavelengths of the coupling and the probe field are nearly the same. f is the optical transition oscillator strength. I is the intensity of the driving laser. The source of the data is Ref. [31]

w_{opt} (Hz)	w_{spin} (Hz)	Γ (Hz)	γ (Hz)	Δ_{jit} (Hz)
2.0×10^9	30.0×10^3	6.1×10^3	9.0×10^3	1.0×10^6
Γ_0 (Hz)	γ_0 (Hz)	λ (nm)	f	I (W/cm^2)
0.01	2.0×10^3	605.7	0.3×10^{-6}	90

and Ce^{3+}:YPO_4) have large spin broadening which makes the condition $\delta_{p+} = \delta_{p-}$ hardly satisfied. Although lasers with large linewidth (nearly 10 MHz) can be used to overcome this difficulty, it also induces a spin dephasing large enough to shorten the SLP's lifetime. So Ce^{3+}-doped crystals are not suitable for generating the SLP. To sum up, we believe that Pr^{3+}:Y_2SiO_5 and N-V centers in diamond might be the best options. The experimental parameters of these materials are listed in Tables I and II.

Figure 3 shows the SLP in Pr:YSO. The sequence of the fields is shown in Fig. 1(b). The data represent a numerical solution of the wave equations (35) and (36) and the atomic density matrix equations (2)–(10). The width of the inhomogeneous broadening of the spin transition in Pr:YSO is 30 kHz and it plays a so important role in creating SLP that we divide it into 100 terms to calculate the integral in Eq. (26). The width of inhomogeneous broadening on the optical transitions is divided into 50 terms, and it is sufficient enough based on our calculations. As shown in Fig. 3, the SLP only lasts for about 10 μs due to the strong decay process which will be quantified theoretically in the following section.

III. THE DECAY AND DIFFUSION PROCESSES

In this section, we use the theoretical approach developed in the preceding section to investigate the decay and diffusion processes of the SLP in the solid materials. First of all, we would like to solve Eqs. (29)–(36) to get the expression for SLP. By substituting Eqs. (29) and (30) into Eqs. (35) and (36), the wave equations become

$$[(c^{-1} - ig\beta_3)\partial_t + \partial_z - ig\beta_1]\Omega_{p+} = ig(\beta_2 + \beta_4\partial_t)\Omega_{p-},$$
$$[(c^{-1} - ig\beta_3)\partial_t - \partial_z - ig\beta_1]\Omega_{p-} = ig(\beta_2 + \beta_4\partial_t)\Omega_{p+}. \quad (38)$$

TABLE II. The inhomogeneous broadening width of the optical transition w_{opt} and the spin transition w_{spin}, the optical transition oscillator strength f, and the density of the ions N. Here Ce:X and Eu:X stand for the Ce^{3+}- and Eu^{2+}-doped crystals we discuss here. The source of the data is Ref. [31].

	N-V Center	Ce:X	Eu:X
w_{opt} (Hz)	375 G	100 G	40 − 60 G
w_{spin} (Hz)	2.7 k	1 − 10 M	10 k
f	0.1	10^{-4}	10^{-4}
N(cm^{-3})	3×10^{18}	10^{20}	10^{19}

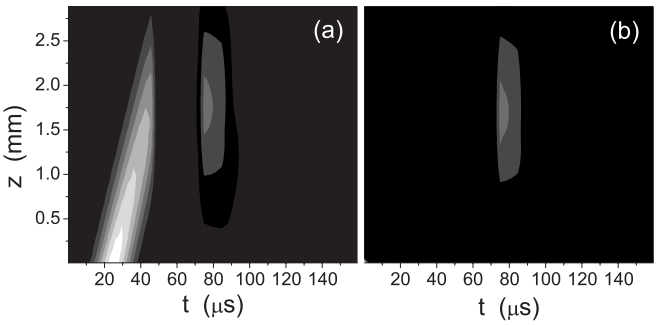

FIG. 3. Numerical simulation of SLP in Pr:YSO. The forward and backward fields are plotted in (a) and (b), respectively. The slow light turning into the coherence of atoms at 45 μs [corresponding to t_1 in Fig. 1(b)] when the forward coupling field is turned off. Both the forward and the backward coupling fields are turned on at 75 μs [corresponding to t_2 in Fig. 1(b)], and the SLP is established. The initial width of the Gaussian wave package is 10 μs. The length of the crystal is 3 mm. The parameters used for the simulation are in Table I.

(39)

Considering the characteristics of Eqs. (38) and (39), we introduce two modes as $\psi_+ = \Omega_{p+} + \Omega_{p-}$, $\psi_- = \Omega_{p+} - \Omega_{p-}$. In terms of these modes the propagation equations read

$$P^{-3}[P^2 g G_{spin} + 2gQ\Omega_c(z,t)\partial_t\Omega_c(z,t)]\psi_+(z,t) + \left[c^{-1} + 2P^{-2}g\Omega_c^2(z,t)\right]\partial_t\psi_+(z,t) = -\partial_z\psi_-(z,t), \quad (40)$$
$$gG_{opt}^{-1}\psi_-(z,t) + c^{-1}\partial_t\psi_-(z,t) = -\partial_z\psi_+(z,t). \quad (41)$$

The parameter Q here takes the form of $G_{spin}G_{opt} - 2\Omega_c^2$. Note that the term of $\partial_z\psi_+$ is close to zero for the small variation of the probe pulse in space. Hence, Eq. (41) is describing the probe pulse-matching process we discussed in the preceding section: ψ_- is absorbed at the rate cgG_{opt}^{-1}. Usually cgG_{opt}^{-1} is much larger than ∂_t, e.g., $cgG_{opt}^{-1} \sim 10^{10}$ in Pr:YSO while the pulse we used in the investigation lasts for about 40 μs, which means $\partial_t \sim 10^7$ in our numerical calculations. This indicates that Ω_{p+} and Ω_{p-} are always matching with each other quickly, therefore ψ_+ can be regarded as the expression of the stationary light pulse. By neglecting $c^{-1}\partial_t$ as compared with gG_{opt}^{-1}, we obtain the zeroth-order solution of ψ_-,

$$\psi_- = -g^{-1}G_{opt}\partial_z\psi_+(z,t). \quad (42)$$

Substituting Eq. (42) into Eq. (40) we obtain

$$\partial_z^2\psi_+(z,t) - \frac{g\left(P^2 + 2cg\Omega_c^2\right)}{cP^2G_{opt}}\partial_t\psi_+(z,t) = \frac{g^2(P^2G_{spin} + 2Q\Omega_c\partial_t\Omega_c)}{P^3G_{opt}}\psi_+(z,t). \quad (43)$$

Here, we focus on step III shown in Fig. 1(b) when the coupling fields become constant after time t_2. Hence we treat $\partial_t\Omega_c$ as zero in Eq. (43). Using the Fourier transformation $\psi_+(z,t) = \sqrt{2/\pi}\int_0^\infty \psi_k(t)\cos(kz)dk$, the expression of $\psi_k(t)$

takes the form of

$$\psi_k(t) = \frac{1}{\sqrt{2a_0}} \exp\left(-\frac{k^2}{4a_0}\right) \times \exp\left(-\frac{cp}{g}\frac{g^2 G_{\text{spin}} + k^2 P G_{\text{opt}}}{P^2 + 2cg\Omega_c^2}\, t\right). \quad (44)$$

We have assumed here that ψ_k has the Gaussian shape $\psi_k(0) = A_0 \exp[-k^2/(4a_0)]$, where A_0 and a_0 are the constant parameters. Then the expression for the SLP takes the form of

$$\psi_+(z,t) = \frac{A_0}{\sqrt{1+J\,t}} \exp\left(-\frac{a_0 z^2}{1+J\,t}\right) \times \exp\left(-\frac{g^2 G_{\text{spin}}}{4a_0 P G_{\text{opt}}} J\, t\right). \quad (45)$$

The parameter $J = 4a_0 c P^2 G_{\text{opt}}/[g(P^2 + 2cg\Omega_c^2)]$ introduced here is just for the simplification of the above equation. As we can see, the decay and diffusion processes can be obtained directly from Eq. (45) and they take the form of

$$D_{\text{dec}} = \exp\left(-\frac{g^2 G_{\text{spin}}}{4a_0 P G_2} J\, t\right), \quad (46)$$

$$D_{\text{dif}} = \frac{1}{\sqrt{1+J\,t}} \exp\left(-\frac{a_0 z^2}{1+J\,t}\right). \quad (47)$$

For the solid materials considered here, the above expressions can be greatly simplified. First, for Pr:YSO, N-V centers in diamond, and Eu^{2+}-doped crystals, the width of the inhomogeneous broadening of low-frequency transition w_{spin} is 1∼10 kHz, while the inhomogeneous broadening of optical transition w_{opt} is modified by the laser linewidth, which can be 1 MHz, and the Rabi frequency of coupling field Ω_c is usually 5 MHz. Therefore, the parameter P defined as $G_{\text{spin}}G_{\text{opt}} + 2\Omega_c^2$ is close to Ω_c^2. Second, to our knowledge, the parameter g is as large as Ω_c (in Pr:YSO) or in the orders of magnitude larger than Ω_c (in N-V centers in diamond), Hence J can be written as $8a_0 g^{-2} G_{\text{opt}}(G_{\text{spin}}G_{\text{opt}} + \Omega_c^2)$ approximately. Based on these two relations, D_{dec} gives a "finite lifetime" T_1 of the SLP corresponding to the decay process:

$$T_1 = \left[G_{\text{spin}}\left(1 + \frac{G_{\text{spin}}G_{\text{opt}}}{2\Omega_c^2}\right)\right]^{-1} \approx \frac{1}{G_{\text{spin}}} - \frac{G_{\text{opt}}}{2\Omega_c^2}. \quad (48)$$

One recognizes the fact that the term G_{spin}^{-1} dominates the lifetime T_1, which indicates that the small decoherence γ_0 and spin broadening w_{spin} can lead to a long-lived SLP in the solid material. The rare-earth ion-doped crystals and N-V centers in diamond have a relatively long-lived spin coherence, e.g., $\gamma_0 = 2$ kHz in Pr:YSO and $\gamma_0 = 25$ kHz in N-V centers in diamond. To our knowledge, there is no certain relationship between the decoherence rate and corresponding inhomogeneous broadening, e.g., $w_{\text{spin}} = 30$ kHz in Pr:YSO and $w_{\text{spin}} = 2.7$ kHz in N-V centers in diamond. However, the total decoherence rates (G_{spin}) of these two materials have the value of the order of 10 kHz, which is relatively small and makes them suitable for the experiment.

D_{dif} describes a typical diffusion process. We integrate D_{dif} over z and obtain $\int D_{\text{dif}} dz = \sqrt{\pi/a_0}$, which is not dependent on t. But the spatial integral of D_{dif}^2 is not a constant: $A(t) = \int D_{\text{dif}}^2 dz = \sqrt{\pi/2a_0(1+Jt)}$. As we know, D_{dif}^2 represents the energy of the pulse or the number of the photons. This indicates that besides the decay process D_{dec}, there is another (nonexponential) decay of the total number of excitation, such a phenomenon in cold atoms (without any inhomogeneous broadening) is studied in Ref. [23]. Here, we would like to introduce another "characteristic time" of the SLP in solids by solving the equation of $A(T_2) = 0.5A(0)$, and obtain

$$T_2 = \frac{3g}{4a_0 c G_{\text{opt}}}. \quad (49)$$

Such a result is under the assumption of the larger coupling Rabi frequency as compared with $G_{\text{opt}}G_{\text{spin}}$ and $\sqrt{cg/2}$ which normally hold for the EIT experiment in solids. As we can see, the parameter G_{opt}, which is the summation of laser linewidth and decoherence of the optical transitions ($G_{\text{opt}} = \gamma + \Delta_{\text{jit}}$), plays an important role in the diffusion process. Based on this, we believe that such a diffusion process (or the nonexponential decay of the pulse) does not result from the decoherence of the spin transition but from the radiative decay and the dephasing process of the optical transition. Because of the relation between the laser linewidth Δ_{jit} and the effective density of the ions N_{eff} as we mentioned in Sec. II, the parameter g which is the function of N_{eff} also depends on laser linewidth Δ_{jit}. The dependence of the SLP in Pr:YSO on the laser linewidth Δ_{jit} (0.5, 0.8, 1.0, 1.5 MHz) is shown in Fig. 4. It is clear that the larger laser linewidth results in the faster nonexponential decay of pulse. We further note here that comparing with T_1 the characteristic time of pulse T_2 is rather large, therefore the lifetime of the pulse is close to T_1.

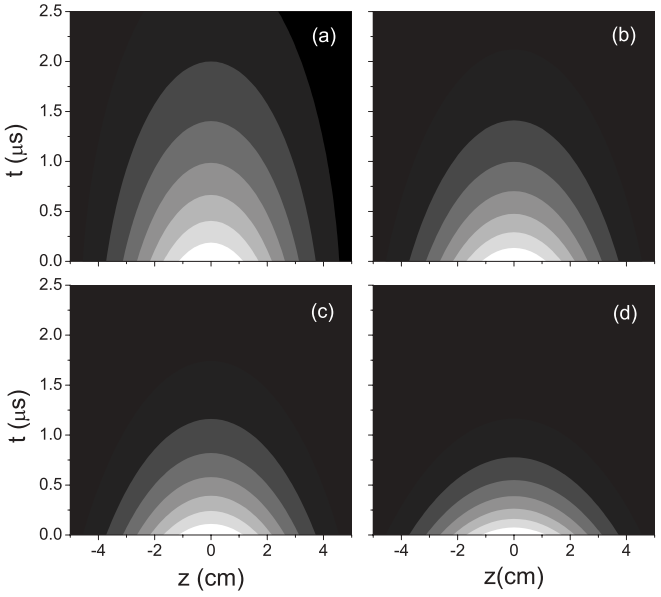

FIG. 4. Stationary light pulse (ψ_+) in Pr:YSO for a laser linewidth of (a) 0.5, (b) 0.8, (c) 1.0, (d) 1.5 MHz. The lighter color in the grayscale maps corresponds to the higher intensity. The Rabi frequency of the coupling field is 5 MHz. The density of Pr^{3+} ions is $4.7 \times 10^{18}\text{cm}^{-3}$. The other parameters are listed on Table I.

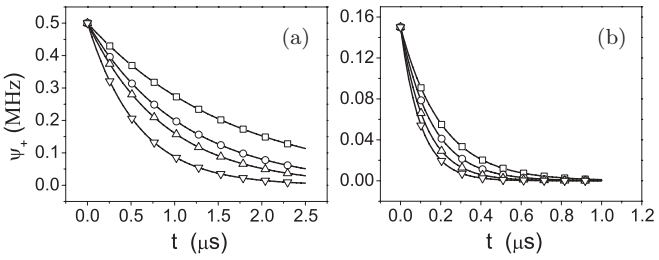

FIG. 5. The amplitude of the stationary light pulse in (a) Pr:YSO and (b) N-V centers in diamond evolving with time t under different laser linewidths: 0.4 (square), 0.6 (circle), 0.8 (up-triangle), and 1.0 (down-triangle). The coupling frequency is the tenfold of $\psi_+(t=0)$. The wavelengths of the SLP are (a) 605 nm and (b) 637 nm. Other parameters are listed in Table II.

Figure 5 shows the amplitude of the SLP in (a) Pr:YSO and (b) N-V centers in diamond crystals under the different laser linewidths. The data are calculated from Eq. (45). As we can see, the lifetime of SLP's in Pr:YSO and N-V centers in diamond crystal are of the same magnitude because the spin broadenings of these materials are both several kilohertz ($w_{\text{spin}} = 30$ KHz for SLP, and 2.7 kHz for N-V centers in diamond). However, the SLP in N-V centers in diamond decays quicker than that in PrYSO; we believe this is because the rather small effective ion density in N-V centers in diamond due to the large optical transition inhomogeneous broadening width (375 GHz). One also notes that the SLP in Pr:YSO is more sensitive to the laser linewidth. This is because its smaller optical broadening width makes the effective ion density more sensitive to the laser linewidth.

Finally, as the answer to the second question we put forth in Sec. I, the decay process of the SLP in the solid is investigated, the decoherence and dephasing rates of both the optical and spin transition are responsible for the lifetime of the SLP, and the precise expression is presented by Eqs. (48) and (49).

IV. CONCLUSIONS

In summary, we investigated the SLP in solid materials with long-lived spin coherence, such as Pr:YSO, N-V centers in diamond, and Eu^{2+}- and Ce^{3+}-doped crystals. The samples are assumed to be a four-level system dressed by a bichromatic SW coupling field so that the counterpropagating Raman excitations can be eliminated. By solving a set of Langevin equations under the effect of the inhomogeneous broadenings modeled by the Lorentzian function, we present the conditions of establishing the SLP in solid materials. Based on such conditions we believe that it is possible to demonstrate SLP in the solid materials we mentioned, especially in Pr:YSO and N-V centers in diamond.

The general expression of the SLP in such solids for the pulses with a small variation of the envelope ($\partial_t \ll cgG_{\text{opt}}^{-1}$) has been obtained. It gives clear descriptions of the decay and diffusion (a nonexponential decay) processes that the SLP in solids undergoes, and also shows that such processes mainly result from the decoherence rate and the inhomogeneous broadenings of the spin and optical transitions, respectively. The inhomogeneous broadenings are the great negative effect base on our calculation. The physical reason, we believe, is that the inhomogeneous broadening which is in the same position of the decoherence rates for both the optical and spin transitions can cause a large dephasing rate. Another parameter that affects the lifetime of the SLP is the laser linewidth, which can be regarded as the broadening of the optical transition as long as the repump scheme is considered. Our research shows that the SLP in Pr:YSO is quite sensitive to the laser linewidth, and the larger laser linewidth always leads to the smaller lifetime of the SLP. The detailed expressions of the characteristic times for both decay and diffusion processes have been presented.

We expect that our general analysis may prompt a more exhaustive understanding of the SLP dynamics in solid materials, and be helpful for experimental research.

ACKNOWLEDGMENTS

The authors would like to acknowledge financial support from the National Basic Research Program (Grants No. 2011CB921603 and No. 2006CB921103) of P. R. China, NSFC (Grants No. 11074097, No. 10774059, and No. 10904048), and Project 20111017 supported by the Graduate Innovation Fund of Jilin University.

[1] S. E. Harris, Phys. Today **50**, 36 (1997).
[2] K. Bergmann, H. Theuer, and B. W. Shore, Rev. Mod. Phys. **70**, 1003 (1998).
[3] C. Y. Ye, V. A. Sautenkov, Y. V. Rostovtsev, and M. O. Scully, Opt. Lett. **28**, 2213 (2003).
[4] L. Wang, X.-L. Song, A.-J. Li, H.-H. Wang, X.-G. Wei, Z. H. Kang, Y. Jiang, and J. Y. Gao, Opt. Lett. **33**, 2380 (2008).
[5] D. A. Braje, V. Balic, G. Y. Yin, and S. E. Harris, Phys. Rev. A **68**, 041801(R) (2003).
[6] H. Kang, G. Hermandez, and Y. Zhu, Phys. Rev. Lett. **93**, 073601 (2004).
[7] Y. P. Zhang, A. W. Brown, and M. Xiao, Phys. Rev. Lett. **99**, 123603 (2007).
[8] S. Li, X. Yang, X. Cao, C. Zhang, C. Xie, and H. Wang, Phys. Rev. Lett. **101**, 073602 (2008).
[9] M. Fleischhauer, and M. D. Lukin, Phys. Rev. Lett. **84**, 5094 (2000).
[10] C. Liu, Z. Dutton, C. H. Behroozi, and L. V. Hau, Nature (London) **409**, 490 (2001).
[11] T. Chaneliere, D. N. Matsukevich, S. D. Jenkins, S.-Y. Lan, T. A. B. Kennedy, and A. Kuzmich, Nature (London) **438**, 833 (2005).
[12] K. S. Choi, H. Deng, J. Laurat, and H. J. Kimble, Nature (London) **452**, 67 (2008).
[13] H. Y. Ling, Y. Q. Li, and M. Xiao, Phys. Rev. A **57**, 1338 (1998).

[14] F. Silva, J. Mompart, V. Ahufinger, and R. Corbalan, Europhys. Lett. **51**, 286 (2000).
[15] F. Silva, J. Mompart, V. Ahufinger, and R. Corbalan, Phys. Rev. A **64**, 033802 (2001).
[16] D. V. Strekalov, A. B. Matsko, and N. Yu, Phys. Rev. A **76**, 053828 (2007).
[17] I.-H. Bae, H. S. Moon, M.-K. Kim, L. Lee, and J. B. Kim, Opt. Express **18**, 1389 (2010).
[18] A. Andre and M. D. Lukin, Phys. Rev. Lett. **89**, 143602 (2002).
[19] X. M. Su and B. S. Ham, Phys. Rev. A **71**, 013821 (2005).
[20] M. Artoni and G. C. La Rocca, Phys. Rev. Lett. **96**, 073905 (2006).
[21] D. Petrosyan, Phys. Rev. A **76**, 053823 (2007).
[22] M. Bajcsy, A. S. Zibrov, and M. D. Lukin, Nature (London) **426**, 638 (2003).
[23] F. E. Zimmer, A. Andre, M. D. Lukin, and M. Fleischhauer, Opt. Commun. **264**, 441 (2006).
[24] J. Otterbach, R. G. Unanyan, and M. Fleischhauer, Phys. Rev. Lett. **102**, 063602 (2009).
[25] J. Otterbach, J. Ruseckas, R. G. Unanyan, G. Juzeliunas, and M. Fleischhauer, Phys. Rev. Lett. **104**, 033903 (2010).
[26] Y.-W. Lin, W.-Y. Liao, T. Peters, H.-C. Chou, J.-S. Wang, H.-W. Cho, P.-C. Kuan, and Ite A. Yu, Phys. Rev. Lett. **102**, 213601 (2009).
[27] B. S. Ham, P. R. Hemmer, and M. S. Shahriar, Opt. Commun. **144**, 227 (1997).
[28] C. Wei and N. B. Manson, Phys. Rev. A **60**, 2540 (1999).
[29] C. Wei and N. B. Manson, J. Opt. B: Quantum Semiclass. Opt. **1**, 464 (1999).
[30] P. R. Hemmer, A. Turukhin, M. S. Shahriar, and J. Musser, Opt. Lett. **26**, 361 (2001).
[31] E. Kuznetsova, O. Kocharovskaya, P. Hemmer, and M. O. Scully, Phys. Rev. A **66**, 063802 (2002).
[32] H.-H. Wang, A.-J. Li, D.-M. Du, Y.-F. Fei, L. Wang, Z.-H. Kang, Y. Jiang, J.-H. Wu, and J.-Y. Gao, Appl. Phys. Lett. **93**, 221112 (2008).
[33] B. S. Ham, Phys. Rev. A **78**, 011808 (2008).
[34] A. V. Turukhin, V. S. Sudarshanam, M. S. Shahriar, J. A. Musser, B. S. Ham, and P. R. Hemmer, Phys. Rev. Lett. **88**, 023602 (2001).
[35] J. J. Longdell, E. Fraval, M. J. Sellars, and N. B. Manson, Phys. Rev. Lett. **95**, 063601 (2005).
[36] H.-H. Wang, X.-G. Wei, L. Wang, A.-J. Li, D.-M. Du, J.-H. Wu, Z.-H. Kang, Y. Jiang, and J.-Y. Gao, Opt. Express **15**, 16044 (2007).
[37] H.-H. Wang, Z.-H. Kang, Y. Jiang, Y.-J. Li, D.-M. Du, X.-G. Wei, J.-H. Wu, and J.-Y. Gao, Appl. Phys. Lett. **92**, 011105 (2008).
[38] H.-H. Wang, D.-M. Du, Y.-F. Fan, A.-J. Li, L. Wang, X.-G. Wei, Z.-H. Kang, Y. Jiang, J.-H. Wu, and J.-Y. Gao, Appl. Phys. Lett. **93**, 231107 (2008).
[39] S. E. Harris, Phys. Rev. Lett. **70**, 552 (1993).